Molecular Simulation Studies on the Adsorption of Mercuric Chloride

R.R. Kotdawala, Nikolaos Kazantzis* and Robert W. Thompson
Department of Chemical Engineering
Worcester Polytechnic Institute
Worcester, MA 01609, USA
*E-mail address: nikolas@wpi.edu

In the present research study, we make an attempt to understand the physical adsorption of mercuric chloride in zeolite NaX and activated carbon through Monte Carlo simulations in the temperature range of 400-500 K. In particular, we consider zeolite NaX with spherical cavities and sodium cations, as well as activated carbon with slit carbon pores and hydroxyl, carboxyl, and carbonyl sites. The capacity and affinity of zeolite NaX are compared with activated carbon with different acid sites by explicitly assessing the impact on mercuric chloride adsorption of a range of magnitudes of the electrostatic interactions considered, namely charge–induced dipole and charge–quadrupole interactions, as well as dispersion interactions.

1. INTRODUCTION

The Clean Air Act amendments identify a number of hazardous air pollutants (HAPs) of particular concern to human health and the environment. Data suggest that coal-fired power plants and municipal solid waste (MSW) incinerators are a significant source of some of these compounds, particularly elemental mercury and mercuric chloride. In the combustion zone, all mercury in coal is vaporized yielding vapor concentrations of mercury in the range of 1-20 μg/m^3 (0.1-2 ppbv). At flame temperatures (1700 K), all of the mercury is expected to be as elemental mercury in the gas phase. In the post flame region (1700-400 K), equilibrium predicts the oxidation of Hg^0 to $HgCl_2$ in the gas phase. Measurements in pilot and full-scale systems show that 10-80 % of the vapor phase mercury is likely to be $HgCl_2$ which is more easily removed from flue gas streams than elemental mercury [1,2,3].

These emissions of mercuric chloride from MSW incinerators and coal burning power plants can be reduced by adsorption on dry sorbents, which can be carried out either by injecting the sorbents into the exhaust gases, or by using multistage fixed beds for selective adsorption of acid gases, mercuric chloride and dioxins [1,2]. Processes which use adsorption on dry sorbents do not pose the problem of the treatment and stabilization of waste liquid streams, and therefore seem very attractive for both small and large combustors such as those used for incineration of hospital wastes for example [1,2,3]. The need to develop technologies capable of achieving high removal efficiencies for mercuric chloride emission control led many researchers to focus their attention on the evaluation of the adsorption capacity and selectivity shown by different solids. Selections of appropriate adsorbent compel researchers to understand the adsorption behavior of mercuric chloride at the molecular level.

The next section provides the requisite information on the particular simulation models proposed for zeolite NaX and activated carbon, followed by a description of the Grand Canonical Monte Carlo (GCMC) simulation scheme employed in the present research study. Finally, Section 4 discusses the simulation results derived.

2. MODEL DESCRIPTIONS

2.1 Zeolite NaX Model

Zeolite NaX was modeled by considering the zeolite cavity as spherically shaped with sodium cations located uniformly in the cavity [4]. The locations of sodium cations were taken from Karavias et al. [4]. The interactions with spherical cavity were calculated using a spherically–averaged potential for the dispersion and repulsion given by [4]:

$$\psi^{disp} = 4C\varepsilon_{1s}\left[\left(\frac{\sigma_{1s}}{R}\right)^{12} L\left\{\frac{r^2}{R^2}\right\} - \left(\frac{\sigma_{1s}}{R}\right)^{6} M\left\{\frac{r^2}{R^2}\right\}\right] \quad (1)$$

where,

$$L\{x\} = (1+12x+25.2x^2+12x^3+x^4)/(1-x)^{10} \quad (2)$$

$$M\{x\} = (1+x)/(1-x)^4 \quad (3)$$

with, $x = \frac{r}{R}$

and ψ^{disp} being a function of r, the radial distance of the adsorbed molecule from the center of the cavity. The cavity radius R was chosen as the distance from the center to the nearest oxygen atom. For zeolite NaX, the cavity radius(R) is 7.057 Å [5]. In the above expression, $C\varepsilon_{1s}$ and σ_{1s} are the Lennard-Jones energy and collision diameter of molecule i with the solid wall respectively. The interactions of mercuric chloride with sodium cations are mainly cation-induced dipole and cation-quadrupole moment

 Cleantech 2007, ISBN 1-4200-6382-0

interactions which can be calculated using equations (4) and (5) respectively, as shown below [6]:

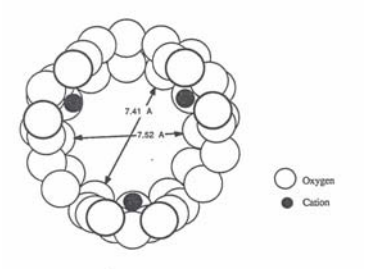

Fig. 1 Cross-section of a zeolite NaX adsorption cavity [4]

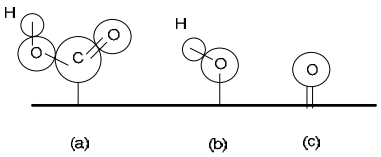

Fig. 2 Schematic representation of the surface sites on carbon: (a) a carboxyl group, (b) a hydroxyl group, and (c) a carbonyl group

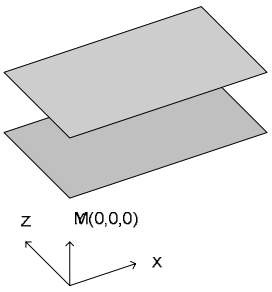

Fig. 3 A schematic diagram of a slit pore with origin at M(0,0,0)

$$\psi^{ind} = -\frac{\alpha q^2}{2r^4(4\pi\varepsilon_o)^2} \qquad (4)$$

where α is the polarizability of the molecule, q is the electronic charge of the ion on the surface, ε_o is the permittivity of vacuum. R is the distance between the centers of the interacting pair [6]. Notice, that interactions between the ion field and the point dipole is given by [6]:

$$\psi^{quadrupole} = -\frac{Qq(3\cos^2\theta - 1)}{4r^3(4\pi\varepsilon_o)} \qquad (5)$$

where, Q is the linear quadrupole moment of the molecule, and θ is the angle between the direction of the field and the axis of the quadrupole.

It should be pointed out, that two types of interactions are considered in the present study, namely dispersion interactions and quadrupole-quadrupole interactions given by Eqns. (4) and (5). The following adsorbate (i)-adsorbate (j) interactions also were considered [7,8]:

$$U_{ij}^{QQ} = \frac{3Q_iQ_j}{4r^5}\left(\begin{array}{l}1-5\cos^2\theta_i-5\cos^2\theta_j+17\cos^2\theta_i\cos^2\theta_j+2\sin^2\theta_i\sin^2\theta_j\cos^2\phi_{ij}\\-16\cos\theta_i\cos\theta_j\sin\theta_i\sin\theta_j\cos\phi_{ij}\end{array}\right) \qquad (6)$$

$$U_{ij}^{disp}(r) = \left[-\frac{1}{(4\pi\varepsilon_0)^2 r_{ij}^6}\left(\frac{3\alpha_i\alpha_j\ (I_i+I_j)}{I_iI_j4}\right)\right] \qquad (7)$$

where I_i and I_j are the first ionization potentials for molecules i and j, respectively.

2.2 Activated Carbon Model

The pores of activated carbon were modeled by considering two parallel walls, each of which comprises an infinite number of layers of graphite. The graphite layers are composed of Lennard- Jones sites, but these are smeared out uniformly over each layer. The interaction between an adsorbate molecule and this smooth carbon surface is represented by the 10-4-3 potential of Steele [9]. Three types of polar surface sites: hydroxyl, carboxyl, and carbonyl groups, were considered in the simulations, and are represented schematically in Fig. 2. The carboxyl, hydroxyl, and carbonyl sites can be considered as a collection of five, two and three point charges. The parameters (size of charge atom and partial charge) of point charges and their positions were taken from Jorge et al. [10]. Cross–species parameters were calculated using the Lorentz-Berthelot combining rule [10]. As mentioned earlier, the electrostatic interactions namely charge-induced dipole moment and charge-quadrupole moment were calculated using equations (4) and (5), respectively.

3. SIMULATION METHODS

We calculated adsorption isotherms using grand canonical Monte Carlo (GCMC) simulations, in which the temperature (T), volume (V), and chemical potentials (μ) were kept constant. The algorithm for GCMC simulations is well documented [11,12], and we used the general methodology. The pressure (P) was calculated from the chemical potential and the equation of state for an ideal gas, and all simulations were performed in equilibrium bulk gas temperature in the range of 400-500 K. Each type of Monte Carlo trial (creation, destruction, and displacement/rotation) was chosen randomly with the same probability. The number of equilibrium steps in the simulations varied

according to the operating conditions, in the range of 30 to 70 millions. During the sampling period, typical configurations for each run were stored in files and then converted into images. In the case of zeolite NaX, the interactions with molecules in four neighboring cavities also were considered. The molecules in the neighboring cavities were the images of molecules in the central cavity. In the case of activated carbon slit pores, we used rectangular simulation cells, bound in the Y direction by pore walls and replicated in X and Z directions using periodic boundary conditions. In order to account for the long range interactions, especially charge–quadrupole, charge-induced dipole and quadrupole–quadrupole interactions, the interactions of molecules in the central cavity with neighboring cavities were considered. The size of the simulation box was 3.0x1.5x3nm.

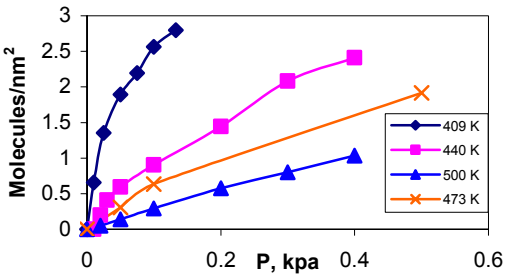

Fig. 4 Adsorption isotherm from GCMC simulation for $HgCl_2$ in zeolite NaX

4. RESULTS AND DISCUSSION

4.1 Adsorption in zeolite NaX

GCMC calculations of mercuric chloride adsorption in zeolite NaX in the temperature range of 409-500 K are shown in Fig. 4, up to an operating pressure of 0.6 kPa. The sorption capacity was predicted to decrease with temperature, as expected. In order to understand the phenomena, the interaction energies of the molecules with the zeolite cavity, sodium cations, and with other mercuric chloride molecules were studied, and are shown in Fig. 5. The figure indicates that the Na–quadrupole moment and fluid-wall dispersion interactions with the spherical cavity dominate over the Na-induced dipole and other interactions among mercuric chloride molecules. In fact, the Total Energy is almost completely due to the Total fluid-wall energy, comprised of the Na-quadrupole, the fluid-wall dispersion, and the Na-induced dipole. However, the Na-induced dipole only plays a minor role in this total.

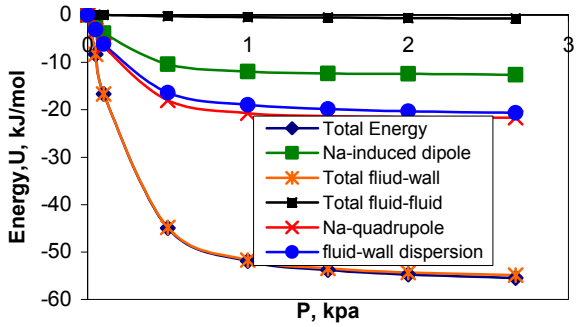

Fig. 5 Relative energy contributions to adsorption for zeolite NaX at 473 K

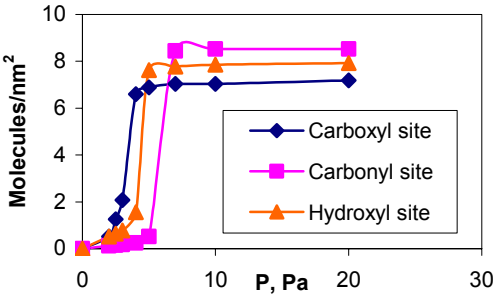

Fig. 6 Adsorption isotherms for activated carbon with acid site concentration of 2.2 sites/nm^2 at 500 K

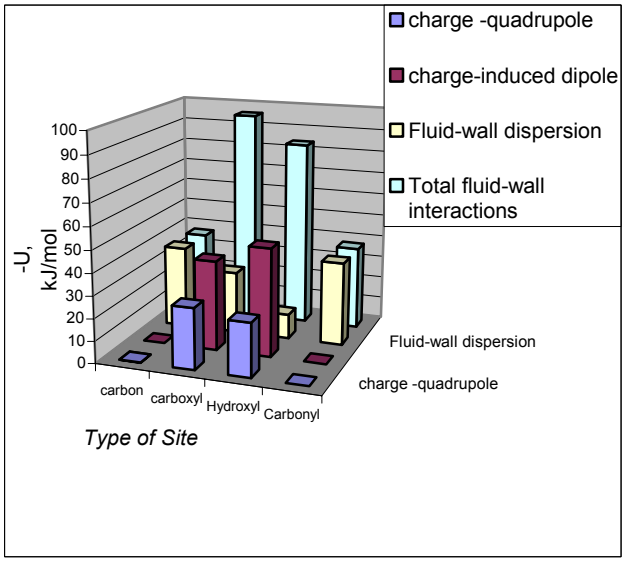

Fig. 7 Relative interaction energy for $HgCl_2$ – activated carbon as a function of acid site at 2 Pa and 450 K

The higher quadrupole interaction is attributed to a high quadrupole moment [13] (-1.48 x 10^{-39} C.m^2) of the molecule, and dispersion interactions might be attributed to the high polarizability (9 $Å^3$) of the molecule [14].

4.2 Adsorption in Activated Carbon

The simulations were carried out by introducing two carboxyl, hydroxyl, and carbonyl functional sites in

Cleantech 2007, ISBN 1-4200-6382-0

the slit pore as well as in the absence of functional sites. The two sites are located at (0.5,1.5,0.5 nm) and (0.5,1.5,1 nm), with the origin M as shown in Fig.3, and correspond to a carbon atom of the functional site that is also a part of the carbon base of the slit pore. The coordinates of the other atoms in the functional sites can be obtained from the bond length and bond angle among them as shown by Jorge et al. [10]. The isotherms for each functional site at 500 K are depicted in Fig. (6). The pore with the carboxyl sites has the highest Henry's Law constant (slope of isotherm in the Zero pressure limit) followed by those with hydroxyl and carbonyl sites. The isotherms also give an indication of a sudden pore filling, implying that the strength of the interactions among mercuric chloride molecules and interactions with the functional sites and the carbon base are comparable. However, the densities of the molecules were low in the case of carboxyl and hydroxyl sites as compared to carbonyl groups. This might be attributed to less available space for the molecule in the pore, due to the greater size of the carboxyl site, indicating the trade off between affinity for the surface and capacity of the adsorbent.

Fig. 7 gives insights of the relative strengths of the interactions with different functional sites and without any functional site. It indicates that the presence of a carbonyl site doesn't increase the affinity to the adsorbate molecules, since the charge-quadropole and charge-induced dipole interactions (electrostatic interactions) are negligible. However, in the case of carboxyl and hydroxyl sites, the electrostatic interactions are greater than dispersion interactions, which would lead to higher affinity for mercuric chloride.

5. CONCLUSIONS

We carried out GCMC simulations to study adsorption phenomena of mercuric chloride molecules in zeolite NaX and activated carbon with and without functional groups. The results from zeolite NaX implies that the Na-quadrupole and dispersion interactions dominate over other types of interactions, suggesting that by manipulating cation density, or types, one can enhance the sorption of the molecule. The evaluation of the sorption of the molecule in activated carbon showed that hydroxyl and carboxyl sites are more important than carbonyl sites. The carboxyl sites give superior affinity than the other two types of functional sites at the expense of the adsorbent's capacity.

References

[1] B. Hall, O.Lindquvist, and E.Ljungstrom, *Env. Sci. Techn*., **24**, 108 (1990)

[2] S.V. Krishnan, B.K. Gullett and W. Jozevicz, *Env. Sci. Techn*., **28**, 1506 (1994)

[3] D. Karatza, A. Lancia, D. Musmarra, F.Pepe and G.Volpicelli, *Comb. Sci. Tech.*, **112**, 163 (1996)

[4] F. Karavias, *Ph.D Thesis*, Univ. of Pennsylvania (1992)

[5] J.L. Soto,and A.L.Myers, *Mol.Phys.*, **42,** 971(1981)

[6] R.T .Yang , *Adsorbents: Fundamentals and applications*, Wiley – Interscience (2003)

[7] T.M. Reed, and K.E. Gubbins, *Applied Statistical Mechanics*, Mc-Graw Hill, NewYork, (1973)

[8] J.M.Prausnitz, R.N. Lichtenthaler and E. Gomes de Azevedo, *Molecular Thermodynamics of Fluid-Phase Equilibria*, 3rd ed, Prentice-Hall, NJ (1999)

[9] W A Steele, *The Interaction of gases with Solid surfaces*, Pergamon Press, Oxford (1974)

[10] M. Jorge, C. Schumacher and N..A. Seaton, *Langmuir*,**18**, 9296 (2002)

[11] D. Frenkel and B. Smit, *Understanding Molecular simulation*, Academic Press, London (1996)

[12] M P Allen and D J Tildesley , *Computer simulation of Liquids*, Clarendon Press: Oxford (1989)

[13] A.N. Pandey, A. Bigotto and .K.Gulati, *Acta Phys. Polon. A*, **80,** 503 (1991)

[14] K.Watanabe, *J. Chem. Phys.* **26**, 542 (1957)